

^7Li NMR Studies of LiCrO_2

Yutaka ITOH*

*Department of Physics, Graduate School of Science, Kyoto Sangyo University,
Kamigamo-Motoyama, Kika-ku, Kyoto 603-8555, Japan*

(Received September 30, 2013)

We report on ^7Li NMR studies of a spin $S = 3/2$ triangular lattice antiferromagnet LiCrO_2 (Néel temperature $T_N = 62$ K) in the paramagnetic state by using the free-induction decay of ^7Li nuclear magnetization. We observed critical divergence of the ^7Li nuclear spin-lattice relaxation rate $1/T_1$ near T_N , a narrow critical region, and a critical exponent $w = 0.45$ from a fit of $1/T_1 \propto (T/T_N - 1)^{-w}$. Although spin frustration effects have been explored for this system, the dynamical critical phenomena suggest that LiCrO_2 in the critical region is a poor low dimensional antiferromagnetic system.

KEYWORDS: spin frustration effect, NMR, LiCrO_2

1. Introduction

LiCrO_2 is a quasi-two dimensional triangular lattice Heisenberg antiferromagnet with a Néel temperature $T_N \approx 62$ K. The crystal structure is an ordered rock salt structure, where the Cr^{3+} ion carries a local moment of $S = 3/2$ on the triangular lattice. Non Curie-Weiss behavior of the uniform spin susceptibility below about 450 K suggests a low dimensional exchange network and a possible spin frustration effect. The Weiss temperature Θ is estimated to be -700 K from the Curie-Weiss susceptibility fit above about 450 K [1]. The spin frustration effects on the paramagnetic state and the magnetic ordered state have been explored by using ESR [2], neutron diffraction [3], NMR and thermodynamic properties [4] and muon spin rotation (μSR) [5]. The temperature dependences of the ESR line width [2] and ^7Li NMR spin-echo relaxation rate [4] were associated with an exponential increase of thermally excited Z_2 vortices (topological defects) [6]. However, three dimensional magnetic structure with double- Q 120° ordering vectors has been observed in the neutron diffraction [3] and μSR [5]. Two dimensional renormalized classical spin correlation also yields an exponential divergence toward $T = 0$ K in the NMR relaxation rate for a triangular lattice Heisenberg antiferromagnet such as Li_7RuO_6 [7]. There remains to be solved whether the two dimensional spin correlation predominates in the paramagnetic state of LiCrO_2 . We have performed a detailed ^7Li NMR experiment using the free induction decay (FID) of ^7Li nuclear magnetization for LiCrO_2 .

In this paper, we report on ^7Li NMR studies of LiCrO_2 polycrystalline samples in the paramagnetic state. We observed critical divergence of the ^7Li nuclear spin-lattice relaxation rate $1/T_1$ near T_N , a narrow critical region, a critical exponent $w = 0.45$ by a fit of $1/T_1 \propto (T/T_N - 1)^{-w}$, and no regimes of the two dimensional renormalized classical spin correlation.

2. Experiments

Powder samples of LiCrO_2 have been synthesized by a conventional solid-state reaction method. Appropriate amounts of Li_2CO_3 and Cr_2O_3 were mixed, palletized and fired at 1150°C for 24 hours

*E-mail address: yitoh@cc.kyoto-su.ac.jp

in air. The products were confirmed to be in a single phase from measurements of the powder X-ray diffraction patterns. A phase-coherent-type pulsed spectrometer was utilized to perform the ${}^7\text{Li}$ NMR (nuclear spin $I = 3/2$) experiments in an external magnetic field of 1.00 T. The NMR frequency spectra were obtained from Fourier transformation of the ${}^7\text{Li}$ FID signals. ${}^7\text{Li}$ nuclear spin-lattice relaxation curves ${}^7p(t) = 1 - F(t)/F(\infty)$ (recovery curves) were obtained by using an inversion recovery technique as a function of time t after an inversion pulse, where FID $F(t)$, $F(\infty)[\equiv F(10T_1)]$ and t were recorded.

3. Results

Figure 1(a) shows the Fourier-transformed (FT) spectra of ${}^7\text{Li}$ FID signals in LiCrO_2 at 77 and 289 K at a reference frequency of 16.5520 MHz. The NMR line of LiClaq represents the reference frequency at zero shift at 1.00 T. No appreciable change is found in the linewidth of the NMR spectra from 289 K to 77 K. The effects of relocation of the Li ions and the motion, which were suggested by the μSR studies [5], could not be found in the NMR spectra of our samples.

Figure 1(b) shows the recovery curves ${}^7p(t)$ of ${}^7\text{Li}$ NMR FID signals as a temperature is decreased. The solid lines are the results from the least-squares fit by a single exponential function

$${}^7p(t) = p(0)\exp\left(-\frac{t}{{}^7T_1}\right) \quad (1)$$

where $p(0)$ and the ${}^7\text{Li}$ nuclear spin-lattice relaxation time 7T_1 are the fit parameters.

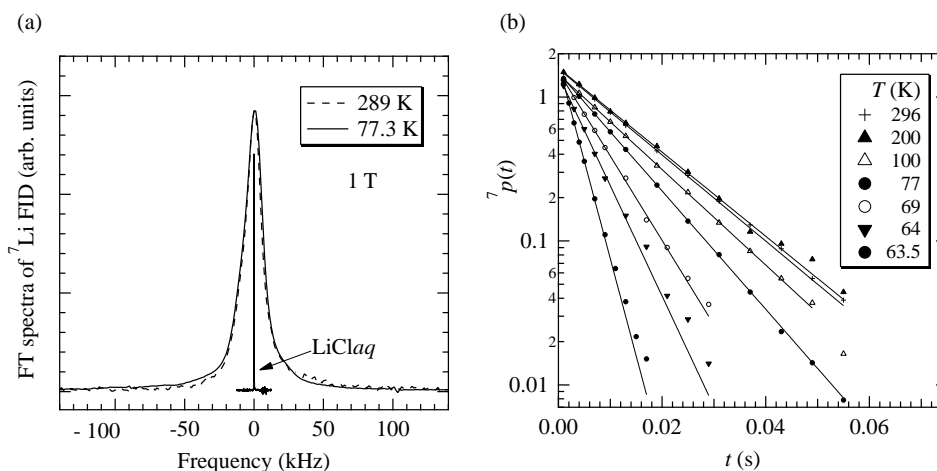


Fig. 1. (a) Fourier-transformed (FT) spectra of ${}^7\text{Li}$ FID signals in LiCrO_2 at 77 and 289 K. (b) Recovery curves ${}^7p(t)$ of ${}^7\text{Li}$ NMR FID signals. Solid lines are the results from the least-squares fit by a single exponential function with a time constant 7T_1 .

Figure 2(a) shows the temperature dependence of $1/{}^7T_1$. With cooling down, $1/{}^7T_1$ shows a critical divergence near T_N , while it levels off at higher temperatures above about 200 K. The high temperature value of $1/{}^7T_{1\infty}$ is estimated to be 69 s^{-1} . The paramagnetic state above about 200 K is in the exchange narrowing limit. Then, the upper limit of an exchange coupling constant J is ~ 200 K. The Curie-Weiss spin susceptibility fit at higher temperatures indicates $J = 80$ K [1, 4].

Figure 2(b) shows normalized $(1/{}^7T_1)/(1/{}^7T_{1\infty})$ versus reduced temperature $|T - T_N|/T_N$. The solid line is the result from the least-squares fit by $1/T_1 = (C/{}^7T_{1\infty})(T/T_N - 1)^{-w}$ where C and w

are the fit parameters. The critical exponent is estimated to be $w = 0.45$. A mean field theory for a three dimensional isotropic Heisenberg antiferromagnet leads to $w = 1/2$ [8]. A dynamic scaling theory indicates $w = 1/3$ for a three dimensional isotropic Heisenberg model [9] and $w = 2/3$ for a three dimensional uniaxial anisotropic Heisenberg model [10]. The exponent of $w = 0.45$ suggests that LiCrO_2 in the critical region is described by a three dimensional interaction model.

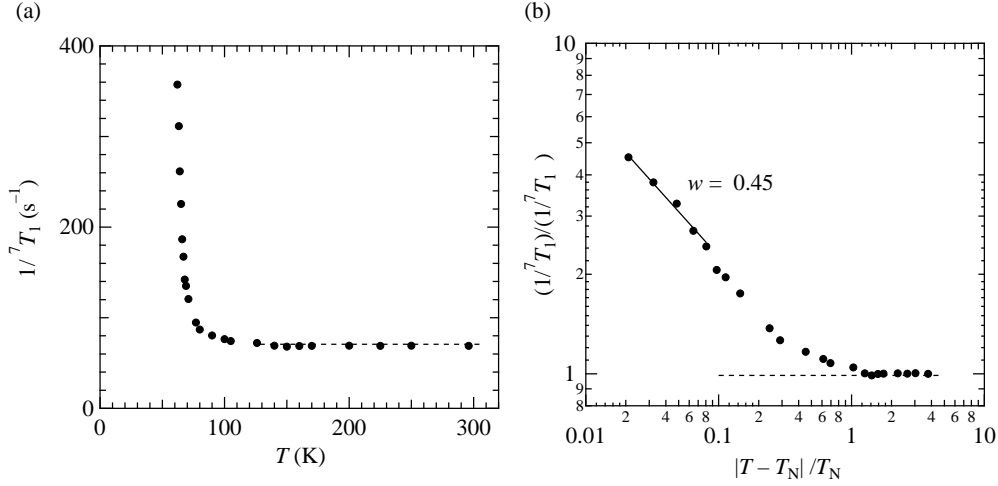


Fig. 2. (a) $1/T_1$ against temperature. $1/T_1$ shows a critical divergence near T_N . The dashed line indicates $1/T_{1\infty} = 69 \text{ s}^{-1}$. (b) Normalized $(1/T_1)/(1/T_{1\infty})$ against reduced temperature $|T - T_N|/T_N$. The solid line indicates $1/T_1 = (T/T_N - 1)^{-w}$.

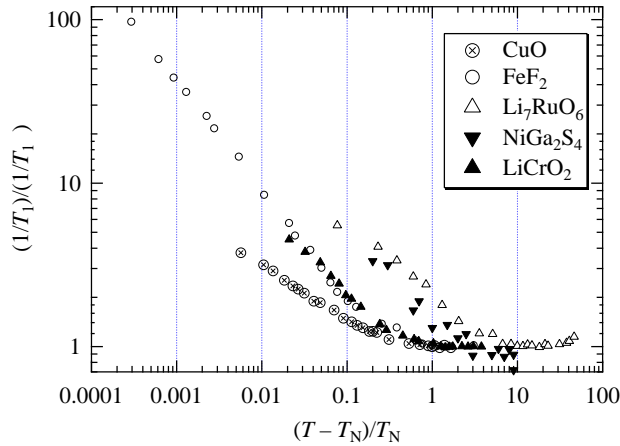


Fig. 3. Normalized $(1/T_1)/(1/T_{1\infty})$ against reduced temperature $(T - T_N)/T_N$ for three dimensional (CuO [11], FeF₂ [12]), triangular-lattice (Li₇RuO₆ [7], NiGa₂S₄ [13]) and the present LiCrO₂.

Figure 3 shows log-log plots of the normalized $(1/T_1)/(1/T_{1\infty})$ against the reduced temperature $(T - T_N)/T_N$ for three dimensional antiferromagnets (CuO [11], FeF₂ [12]), triangular-lattice antiferromagnets (Li₇RuO₆ [7], NiGa₂S₄ [13]) and the present LiCrO₂. The critical divergence of

$(1/T_1)/(1/T_{1\infty})$ of LiCrO_2 coincides with a part of FeF_2 , which is a uniaxial anisotropic Heisenberg system. The onset of the increase in the NMR relaxation rate near T_N empirically categorizes the critical region. The region of $|T - T_N|/T_N \leq 10$ has been assigned to the renormalized classical regime with the divergent spin-spin correlation length toward $T = 0$ K [7]. The region of $|T - T_N|/T_N \leq 1.0$ has been assigned to the three dimensional critical regime with the divergent spin-spin correlation length toward T_N . Thus, the narrow critical region of $|T - T_N|/T_N \leq 1$ also indicates that LiCrO_2 is in the three dimensional critical regime.

4. Discussions

The theoretical analysis of the non-linear sigma model for the spin S frustrated quantum antiferromagnets gives us the magnetic correlation length [14–17]

$$\xi \propto \frac{1}{\sqrt{T}} \exp(4\pi\rho_s/T) \quad (2)$$

with a spin stiffness constant ρ_s and the nuclear spin-lattice relaxation rate

$$\frac{1}{T_1 T^3} \propto \exp(4\pi\rho_s/T). \quad (3)$$

Here, the spin stiffness constant ρ_s is expressed by

$$\rho_s = \frac{\sqrt{3}}{2} Z_s S^2 J_s, \quad (4)$$

where a renormalization factor Z_s is calculated by a spin-wave approximation and $1/S$ expansion and J_s is the nearest neighbor exchange coupling constant [18].

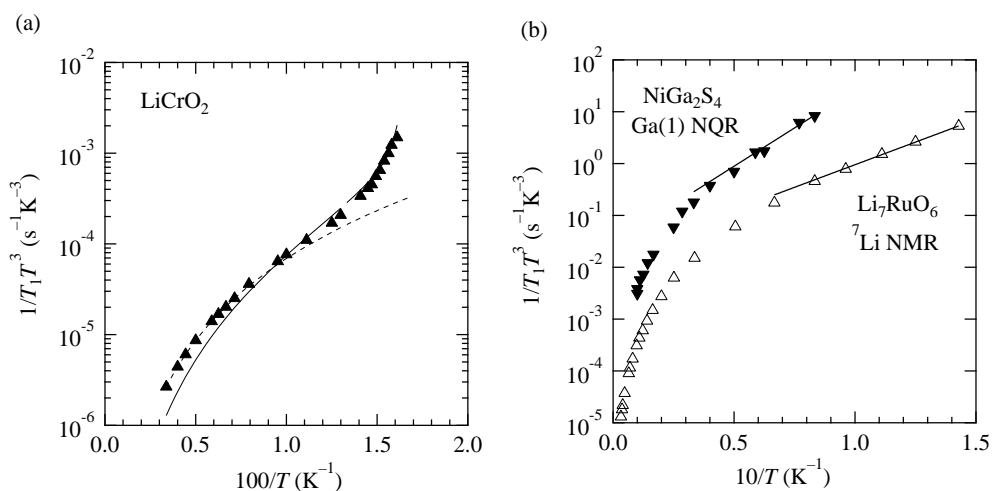


Fig. 4. (a) Semi-logarithmic plot of $1/T_1 T^3$ against inverse temperature $100/T$ for LiCrO_2 . The dash curve indicates $1/T_1 = 1/T_{1\infty}$. The solid curve indicates $1/T_1 \propto (T/T_N - 1)^{-w}$. (b) Semi-logarithmic plots of $1/T_1 T^3$ against inverse temperature $10/T$ for Li_7RuO_6 [7] and NiGa_2S_4 [13]. The solid lines indicate $1/T_1 T^3 \propto \exp(4\pi\rho_s/T)$.

Table I. Spin stiffness constants and exchange coupling constants estimated from the analysis using the two dimensional renormalized classical model for triangular lattice compounds. The data of Li_7RuO_6 are reproduced from ref. [7]. The data of NiGa_2S_4 are estimated from Fig. 4(b) using the experimental T_1 values in ref. [13]. The data of KCrO_2 are reproduced from ref. [19]. J_Θ of LiCrO_2 is from refs. [1, 4].

	$4\pi\rho_s$ (K)	J_s (K)	J_Θ (K)
Li_7RuO_6	40	2.1	9.7
NiGa_2S_4	68	9.5	20
KCrO_2	130	9.3	29
LiCrO_2	—	—	80

Figure 4(a) shows semi-logarithmic plot of $1/T_1 T^3$ against inverse temperature $100/T$ for LiCrO_2 . The dash curve is $1/T_1 = 1/T_{1\infty}$. The solid curve is a best fit result of $1/T_1 \propto (T/T_N - 1)^{-w}$ near T_N . No trace of two dimensional renormalized classical regime is found.

For comparison, Fig. 4(b) shows semi-logarithmic plots of $1/T_1 T^3$ against inverse temperature $10/T$ for Li_7RuO_6 [7] and NiGa_2S_4 [13]. The solid lines are the best fit results of $1/T_1 T^3 \propto \exp(4\pi\rho_s/T)$, which is characteristic of the two dimensional renormalized classical behavior of the triangular lattice spin systems.

Since the solid lines in Fig. 4(b) well fit the experimental $1/T_1$ at low temperatures, the spin-spin correlations of Li_7RuO_6 [7] and NiGa_2S_4 [13] are in the two dimensional renormalized classical regimes. However, the exchange coupling constants J_s 's estimated from eqs. (2) and (3) are smaller than the exchange constants J_Θ 's estimated from the Curie-Weiss susceptibility fit at higher temperatures [20]. The estimated parameters of $4\pi\rho_s$, J_s and J_Θ are listed in Table 1. One may find $J_s \sim J_\Theta/5$ for Li_7RuO_6 , $J_s \sim J_\Theta/2$ for NiGa_2S_4 , and $J_s \sim J_\Theta/3$ for KCrO_2 . Since no frustration effects are taken into consideration in eq. (3), the reason of $J_s < J_\Theta$ can be traced back to the spin frustration effects on a spin-spin correlation function at a low frequency. Actually, the reduction of the spin stiffness constant ρ_s due to the spin frustration (\mathbb{Z}_2 vortices) is seen in the numerical studies of Heisenberg frustrated spin systems [21].

5. Conclusions

We have made a detailed experimental study of the ^7Li NMR FID signal in the paramagnetic state of the triangular lattice antiferromagnet LiCrO_2 . The critical behavior of the ^7Li nuclear spin-lattice relaxation rate $1/T_1$ of the FID signal near T_N is found to be well described by a power law. The critical exponent takes $w = 0.45$. The narrow critical region and no trace of two dimensional renormalized classical regime are found. The three dimensional exchange interaction may play a central role in the critical behavior of LiCrO_2 .

References

- [1] C. Delmas, G. Le Flem, C. Fouassier and P. Hagenmuller: J. Phys. Chem. Solids **39** (1978) 55.
- [2] Y. Ajiro, H. Kikuchi, S. Sugiyama, T. Nakashima, S. Shamoto, N. Nakayama, M. Kiyama, N. Yamamoto and Y. Oka: J. Phys. Soc. Jpn. **57** (1988) 2268.
- [3] H. Kadowaki, H. Takei and K. Motoya: J. Phys.: Condens. Matter **7** (1995) 6869.
- [4] L. Alexander, N. Büttgen, R. Nath, A. Mahajan and A. Loidl: Phys. Rev. B **76** (2007) 064429.
- [5] J. Sugiyama, M. Månsson, Y. Ikedo, T. Goko, K. Mukai, D. Andreica, A. Amato, K. Ariyoshi and T. Ohzuku: Phys. Rev. B **79** (2009) 184411.
- [6] H. Kawamura and S. Miyashita: J. Phys. Soc. Jpn. **53** (1984) 4138.
- [7] Y. Itoh, C. Michioka, K. Yoshimura, K. Nakajima and H. Sato: J. Phys. Soc. Jpn. **78** (2009) 023705.
- [8] T. Moriya: Prog. Theor. Phys. **28** (1962) 371.
- [9] B. I. Halperin and P. C. Hohenberg: Phys. Rev. Lett. **19** (1967) 700.

- [10] E. Riedel and F. Wegner: Phys. Rev. Lett. **24** (1970) 730.
- [11] Y. Itoh, T. Imai, T. Shimizu, T. Tsuda, H. Yasuoka and Y. Ueda: J. Phys. Soc. Jpn. **59** (1990) 1143.
- [12] A. M. Gottlieb and P. Heller: Phys. Rev. B **3** (1971) 3615.
- [13] H. Takeya, K. Ishida, K. Kitagawa, Y. Ihara, K. Onuma, Y. Maeno, Y. Nambu, S. Nakatsuji, D. E. MacLaughlin, A. Koda and R. Kadono: Phys. Rev. B **77** (2008) 054429.
- [14] P. Azaria, B. Delamotte and D. Mouhanna: Phys. Rev. Lett. **68** (1992) 1762.
- [15] P. Azaria, Ph. Lecheminant and D. Mouhanna: Nucl. Phys. B **455** (1995) 648.
- [16] A. V. Chubukov, S. Sachdev and T. Senthil: Phys. Rev. Lett. **72** (1994) 2089.
- [17] A. V. Chubukov, S. Sachdev and T. Senthil: Nucl. Phys. B **426** (1994) 601.
- [18] A. V. Chubukov, S. Sachdev, and T. Senthil: J. Phys.: Condens. Matter **6** (1994) 8891.
- [19] F. Xiao, T. Lancaster, P. J. Baker, F. L. Pratt, S. J. Blundell, J. S. Möller, N. Z. Ali and M. Jansen: arXiv:1307.1377.
- [20] From the analysis using eq. (2) for the muon spin relaxation rate for NiGa₂S₄, the agreement of $J_s \approx J_\Theta = 20$ K is reported in the following reference [S. Zhao, P. Dalmas de Réotier, A. Yaouanc, D. E. MacLaughlin, J. M. Mackie, O. O. Bernal, Y. Nambu, T. Higo and S. Nakatsuji: Phys. Rev. B **86** (2012) 064435]. If the discrepancy between the Ga NQR and μ SR results with respect to the critical divergence is intrinsic, it might show a strong frequency dependence of the slow dynamics characteristic of frustrated systems.
- [21] M. Caffarel, P. Azaria, B. Delamotte, and D. Mouhanna: Phys. Rev. B **64** (2001) 014412.